Heliyon 10 (2024) e31956

Contents lists available at ScienceDirect

Heliyon

journal homepage: www.cell.com/heliyon

Research article

Inactivation of guanylate kinase in *Bacillus* sp. TL7-3 cultivated under an optimized ratio of carbon and nitrogen sources influenced GTP regeneration capability and sporulation

Phetcharat Jaiaue [a], Piroonporn Srimongkol [b,c], Sitanan Thitiprasert [b,c,**], Jirabhorn Piluk [b,c,***], Jesnipit Thammaket [a], Suttichai Assabumrungrat [d], Benjamas Cheirsilp [e], Somboon Tanasupawat [f], Nuttha Thongchul [b,c,*]

[a] *Program in Biotechnology, Faculty of Science, Chulalongkorn University, Bangkok, Thailand*
[b] *Center of Excellence in Bioconversion and Bioseparation for Platform Chemical Production, Institute of Biotechnology and Genetic Engineering, Chulalongkorn University, Bangkok, Thailand*
[c] *Institute of Biotechnology and Genetic Engineering, Chulalongkorn University, Bangkok, Thailand*
[d] *Department of Chemical Engineering, Faculty of Engineering, Chulalongkorn University, Bangkok, Thailand*
[e] *Department of Industrial Biotechnology, Faculty of Agro-Industry, Prince of Songkla University, Songkla, Thailand*
[f] *Department of Biochemistry and Microbiology, Faculty of Pharmaceutical Sciences, Chulalongkorn University, Bangkok, Thailand*

ARTICLE INFO

Keywords:
Bacillus sp. TL7-3
Sporulation
codY
spo0A
Guanylate kinase

ABSTRACT

Bacillus sp. TL7-3 has potential as a dietary supplement to promote human and animal health. It produces spores that can survive in harsh environments. Thus, when supplemented with nutrients, these spores can withstand the acidic pH of the stomach and resume vegetative development in the gut when exposed to growth-promoting conditions. Spores are formed as a cellular defense mechanism when a culture experiences stress and process optimization to achieve high spore production in a typical batch process remains challenging. Existing literature on the manipulation of gene expression and enzyme activity during batch cultivation is limited. Studies on the growth patterns, morphological changes, and relevant gene expression have aided in enhancing spore production. The present study used the response surface methodology for medium optimization. The model suggested that yeast extract and NH_4Cl were significant factors controlling spore production. A comparison between the high weight ratio of carbon and nitrogen (C:N) substrates (8.57:1) in the optimized and basal media (0.52:1) showed an 8.76-fold increase in the final spore concentration. The expression of major genes, including *codY*, *spo0A*, *kinA*, and *spo0F*, involved in the sporulation was compared when cultivating *Bacillus* sp. TL7-3 in media with varying C:N ratios. At high C:N ratios, *spo0A*, *kinA*, and *spo0F* were upregulated, whereas *codY* was downregulated. This led to decreased guanylate kinase activity, resulting in a low guanosine triphosphate concentration and inactivation of CodY, thereby reducing the repression of *spo0A* and CodY-repressed genes and stimulating sporulation.

* Corresponding author.
** Corresponding author.
*** Corresponding author. Center of Excellence in Bioconversion and Bioseparation for Platform Chemical Production, Institute of Biotechnology and Genetic Engineering, Chulalongkorn University, Bangkok, Thailand.
E-mail addresses: Sitanan.T@chula.ac.th (S. Thitiprasert), Nuttha.T@chula.ac.th (N. Thongchul).

https://doi.org/10.1016/j.heliyon.2024.e31956
Received 20 September 2023; Received in revised form 23 May 2024; Accepted 24 May 2024
Available online 25 May 2024

1. Introduction

Bacillus subtilis is a bacterial species that harbors strains with probiotic characteristics. The Food and Drug Administration has designated *B. subtilis* as "Generally Recognized as Safe" for human and animal use because it improves human and animal health by balancing the gut microbiota [1]. Unlike many other bacteria, *B. subtilis* produces spores that facilitate its survival under extreme conditions, such as under conditions of low pH in the digestive tract and high temperatures during food and feed processing. These spores can withstand acidic environments in the stomach and germinate in the gut when conditions become favorable [2]. As spores are produced as part of cellular defense when a culture is exposed to harsh environmental conditions, process control for specific isolates to achieve high spore production remains challenging. In addition, little is known about the manipulation of the spore formation mechanism in *B. subtilis,* making it difficult to achieve high concentrations and yields [3].

Analyses of growth patterns, morphology, and relevant gene expression could lead to improvements in spore production. Sporulation occurs when a culture is exposed to adverse conditions such as malnutrition, causing vegetative cells to begin to turn into spores. The transition occurs in seven stages. In stage 1, cells asymmetrically divide from the tightened Z ring (stage 1). In stage 2, after septum formation, the two daughter cells, the spore mother cell, and the pre-spore are formed. In stage 3, the spore mother cell engulfs the pre-spore. In stages 4 and 5, coated layers such as the cell wall, cell membrane, and cortex are generated by the pre-spore, whereas the spore mother cell causes lysis. In stages 6 and 7, the pre-spore readily transforms into an endospore via lysis and is then released as a free spore. Free spores remain dormant under extreme conditions and resume vegetative growth and cell division via germination when exposed to favorable environmental conditions [4].

In *B. subtilis*, septum production inside vegetative cells during the early stages of sporulation (stage 2) is a major phase that regulates sporulation [5,6]. The key gene responsible for the regulation of this step is *spo0A*. This gene encodes the Spo0A protein, which stimulates a series of sigma (σ) factor proteins that participate in septum formation [7]. Hence, understanding the expression and activation of Spo0A is necessary for manipulating growth patterns and spore production. CodY and intracellular guanosine triphosphate (GTP) regulate Spo0A activation. CodY is a transcriptional suppressor that inhibits the expression of *spo0A*, resulting in a lack of Spo0A protein to activate a series of factors during septum formation [8–10].

Similarly, intracellular GTP binds to the metabolic-binding domain of CodY, resulting in the correct conformation. This leads to the activation of a protein that suppresses *spo0A* transcription. Cells cultured in low-nutrient media have limited intracellular GTP levels. This eventually causes inactivation of CodY and leads to the expression of *spo0A* and subsequent initiation of sporulation [11,12]. The transition from vegetative growth to the dormant stage indicates the beginning of spore production. During spore production, a high spore concentration is obtained because of the high abundance of vegetative cells entering the sporulation process [13,14]. Therefore, sporulation and spore production can be triggered by understanding the culture medium requirements. Vegetative microbes typically enter sporulation when nitrogen sources are limited. Culture medium with a low nitrogen source results in an increase in the carbon-to-nitrogen substrate ratio, which limits early-stage vegetative growth. Understanding vegetative growth kinetics can facilitate a high rate of vegetative growth at an early stage and provide information on the medium requirements. However, knowledge regarding the use of carbon and nitrogen substrates in culture medium to trigger sporulation is limited.

Bacillus spp. are the predominant microorganisms in fermented soybeans. Compared to Japanese natto, traditional Thai fermented soybeans are produced under home manufacturing conditions, leading to the presence of *Bacillus* sp. in the fermented soybean. Therefore, traditional Thai fermented soybeans are a good source of health-promoting substances, including free amino acids, small peptides, bioactive compounds, and enzymes [15–17]. *Bacillus* spp. has significant applications in aquaculture as a probiotic bacterium against *Aeromonas hydrophilia* in Nile tilapia (*Oreochromis niloticus*) [18]. Unlike other probiotic bacteria, *Bacillus* sp. is a spore-forming microbe; and thus, can withstand extreme conditions such as high temperature and low pH. This characteristic enables *Bacillus* sp. to thrive in an acidic environment in the stomach, leading it to germinate, proliferate, and function as a probiotic in the digestive tract [14,15]. As previously stated, process optimization to obtain high spore concentration at a sufficiently high production rate of *Bacillus* sp. is necessary. However, only a few studies on spore production in low-cost media have been conducted [19].

This study isolated *Bacillus* sp. TL7-3 from traditional Thai fermented soybeans and preliminarily identified it as a probiotic bacterium (Tables S1 and S2, Fig. S1 in Supplementary Materials). The present study aimed to investigate sporulation during the cultivation of *Bacillus* sp. TL7-3 in a basal medium containing glucose, yeast extract, and NH_4Cl. Owing to the high cost of conventional sporulation media such as Difco sporulation medium (DSM), basal medium was chosen because it is inexpensive and promotes vegetative growth at an early stage before sporulation [19]. The medium was optimized using response surface methodology (RSM) to enhance spore production. The expression of sporulation-related genes, such as *spo0A*, *codY*, *kinA*, and *spo0F,* was analyzed during growth along with the growth pattern. Guanylate kinase (GK) activity and ratio of spore count to total cell number were also investigated. When the weight ratio of carbon-to-nitrogen substrates was increased, the downregulation of *codY*, upregulation of *spo0A*, *kinA*, and *spo0F*, specific activity of GK, and intracellular guanosine monophosphate (GMP), guanosine diphosphate (GDP), GTP levels indicated the initiation of sporulation and subsequently turned vegetative growth into the dormant stage. This resulted in an increase in spore concentration. The response surface model equation established in this study can be applied to enhance spore production. Additionally, growth and gene expression patterns can be used to determine the process parameters during the cultivation of spore-forming bacteria.

2. Results

2.1. Enhanced spore production by medium optimization

A central composite design (CCD) was used to explain the interactions between glucose, yeast extract, and NH_4Cl during spore production. The ranges and levels of the assigned parameters are listed in Table 1. To evaluate the effect of carbon and nitrogen sources using RSM, the concentrations of glucose, yeast extract, and NH_4Cl in the culture medium were varied using one fixed factor to predefine the threshold for CCD (Figs. S2-S4 in the Supplementary Materials). Glucose, a major carbon skeleton, was varied first. In our approach, the more vegetative cells produced, the higher the number of spores obtained at the end of batch cultivation. Nitrogen sources were also investigated. A high carbon-to-nitrogen ratio during the early growth stages enhances vegetative growth. As fermentation proceeds, the low residual nitrogen and high residual glucose levels trigger sporulation. Therefore, we hypothesized that the concentrations of yeast extract and NH_4Cl affect growth and sporulation. The concentration threshold obtained from one fixed factor was used to define the set of experimental runs by CCD to determine the effects of the three variants. The matrix from the CCD was generated and consisted of 20 factorial designs, including eight axial points (runs 1–8), six star points (runs 9–14), and six center points (runs 15–20), covering the entire range of the three variables in combination (Table 2). The spore concentration obtained from the experimental runs was represented as the actual response, whereas the predicted response was represented by the simulated data generated by the CCD. The dataset of the actual responses that yielded the maximum spore concentration was input into the CCD to generate a model equation. A mathematical model (Design Expert software) that explained spore production as a polynomial function of three independent parameters, glucose (x_1), yeast extract (x_2), and NH_4Cl (x_3), was obtained (Eq. (1)).

$$Y\ (\text{spore concentration}) = -1.60 + 1.01x2\text{-}2.12x3{+}0.02x2x3\text{-}2.83x12\text{-}0.16x22\text{-}0.02 \times 32 \quad (1)$$

The RSM model was statistically tested and the results are listed in Table 3. The F value of 27.17 indicated that the model was significant, confirming its reliability. Furthermore, the model's p-value (0.001) was quite low. The p-values of each coefficient were examined to understand the links between the test variables. Table 3 displays the coefficients and corresponding p-values. The coefficients became more significant when the p-values were lower. The model was considered significant when the p-value was <0.05. From the test results in Table 3, the significant variables are x_2, x_3, x_2x_3, x_1^2, x_2^2, and x_3^2, with x_2x_3 being the most significant.

The coefficient of regression (R^2) was employed to show the fit of the model and the analysis of variance (ANOVA) yielded an R^2 value of 0.9607, suggesting that the model could explain 96.07 % of the variation (Eq. (1)) and indicating strong agreement between the predicted and actual values. Therefore, the model predictions were acceptable. The reliability of the model was determined using the predicted R^2 (0.7825) and adjusted R^2 (0.9253) values. The signal-to-noise ratio was explained by adequate precision, for which the ratio should be greater than four. The precision was 16.004, indicating that the model can be used to navigate the design space. The precision was verified using the coefficient of variation (CV). A higher CV value implies that a study has lower reliability, with values exceeding 30 % indicating caution should be taken regarding the experimental data. In this study, the CV was 7.09 %, indicating good reliability.

2.2. Three-dimensional surface plot to explain sporulation

RSM was used to examine the influence of these three parameters on spore formation by creating three-dimensional (3-D) surface and contour plots. The response surface plot revealed two factors. The other factors were fixed individually to further understand the interaction effects of the two observable parameters. Fig. 1 shows the contour plots and response surface graphs representing the interaction between the two factors simultaneously and the optimal level for each variable (concentrations of glucose, yeast extract, and NH_4Cl). The shape of the contour plot illustrates these interactive effects. Elliptical contour plots were obtained, demonstrating that the variables exhibited good interaction, whereas circular contour plots indicated no interaction between the two variables.

Contour plots revealed that the optimum concentrations of glucose (x_1), yeast extract (x_2), and NH_4Cl (x_3) were 60, 3, and 4 g/L, respectively, with a corresponding weight ratio of carbon-to-nitrogen (C:N) substrates of 8.57 to 1. The highest spore concentration of 1.05×10^8 CFU/mL was obtained after cultivating *Bacillus* sp. TL7-3 in a medium with optimum concentrations of glucose, yeast extract, and NH_4Cl. This spore concentration was approximately 8.76-fold higher than that obtained after the cultivation of *Bacillus* sp. TL7-3 in an unoptimized basal medium containing 10 g/L glucose, 15 g/L yeast extract, and 4 g/L NH_4Cl (weight ratio of C:N substrates of 0.52–1) of 1.20×10^7 CFU/mL. The contour of the 3-D plot explained the effects of the variables on the response. A gentle contour of the surface curve suggests that the variable has no significant influence on the response, whereas an abrupt contour indicates that it has a significant effect on the response. Fig. 1 shows that the spore concentration was affected by the combination of glucose and yeast

Table 1
Variables used in the CCD with experimental range and levels.

Variable	Symbol coded	Range and level				
		−1.68 (−α)	−1	0	+1	+1.68 (+α)
Glucose (g/L)	x_1	26.36	40	60	80	93.64
Yeast extract (g/L)	x_2	1.31	2	3	4	4.68
NH_4Cl (g/L)	x_3	0.64	2	4	6	7.36

Table 2
Experimental design and results of full CCD model representing the levels and ranges of tested variables including glucose (x_1), yeast extract (x_2), and NH_4Cl (x_3) as well as the responses predicted by the model and the actual values obtained from the experimental runs.

Run	Levels and ranges of variables[a]			Response[b]	
	Glucose (x_1)	Yeast extract (x_2)	NH_4Cl (x_3)	Predicted	Actual
1	(-1) 40	(-1) 2	(-1) 2	0.72	0.73
2	(-1) 40	(-1) 2	(+1) 6	0.43	0.44
3	(-1) 40	(+1) 4	(-1) 2	0.70	0.76
4	(-1) 40	(+1) 4	(+1) 6	0.74	0.74
5	(+1) 80	(-1) 2	(-1) 2	0.65	0.65
6	(+1) 80	(-1) 2	(+1) 6	0.51	0.55
7	(+1) 80	(+1) 4	(-1) 2	0.76	0.74
8	(+1) 80	(+1) 4	(+1) 6	0.65	0.72
9	(-1.68) 26.36	(0) 3	(0) 4	0.65	0.60
10	(+1.68) 93.64	(0) 3	(0) 4	0.66	0.66
11	(0) 60	(-1.68) 1.31	(0) 4	0.38	0.33
12	(0) 60	(+1.68) 4.68	(0) 4	0.67	0.64
13	(0) 60	(0) 3	(-1.68) 0.64	0.98	0.85
14	(0) 60	(0) 3	(+1.68) 7.36	0.70	0.70
15	(0) 60	(0) 3	(0) 4	0.98	1.01
16	(0) 60	(0) 3	(0) 4	0.98	0.93
17	(0) 60	(0) 3	(0) 4	0.98	1.06
18	(0) 60	(0) 3	(0) 4	0.98	0.95
19	(0) 60	(0) 3	(0) 4	0.98	0.98
20	(0) 60	(0) 3	(0) 4	0.98	0.98

[a] The values in the blankets indicate the tested levels, and the ranges are the concentrations (g/L) of the tested variables in the fermentation medium.
[b] Predicted responses were the simulated values of spore concentration (CFU/mL) obtained from the CCD model. The actual responses were the spore concentrations (CFU/mL) obtained from the experimental runs.

Table 3
Analysis of variance (ANOVA) for the response surface quadratic model.

Source	Sum of squares	df	Mean square	F value	p value	
Model	0.69	9	0.077	27.17	<0.0001	Significant
x_1	6.051×10^{-4}	1	6.051×10^{-4}	0.21	0.6539	
x_2	0.090	1	0.090	31.92	0.0002	
x_3	0.034	1	0.034	12.03	0.0060	
x_1x_2	6.125×10^{-4}	1	6.125×10^{-4}	0.22	0.6519	
x_1x_3	4.513×10^{-3}	1	4.513×10^{-3}	1.59	0.2356	
x_2x_3	0.015	1	0.015	5.40	0.0424	
x_1^2	0.190	1	0.190	65.31	<0.0001	
x_2^2	0.390	1	0.390	137.77	<0.0001	
x_3^2	0.055	1	0.055	19.58	0.0013	
Residual	0.028	10	2.834×10^{-3}			
Lack of fit	0.018	5	3.557×10^{-3}	1.69	0.2903	Not significant
Pure error	0.011	5	2.110×10^{-3}			

Notes: R^2 0.9607.
Predicted R[b] 0.7825.
Adjusted R^2 0.9253.
Adequate precision 16.004.
CV%7.09.

extract, glucose and NH_4Cl, and yeast extract and NH_4Cl.

2.3. Growth and sporulation of Bacillus sp. TL7-3 in response to the weight ratio of C:N substrates

Bacillus sp. TL7-3 cells were grown in three different media (basal medium, optimized medium, and DSM) to compare growth and sporulation patterns (Figs. 2–4). The growth curves and spore-forming characteristics of both media were examined during culturing. The total and vegetative cell counts of *Bacillus* sp. TL7-3 cells cultured on non-optimized basal medium were almost the same, whereas the spore numbers were approximately 10 times lower than the vegetative cell counts (Fig. 2A). In contrast, most vegetative cells grown in the optimized medium entered sporulation and formed spores at a later stage of cultivation (Fig. 3A). Cell morphology was observed under a microscope (Fig. 2B and 3B). Malachite green and safranin O were used to stain the cell samples. The spores were stained green, whereas the vegetative cells were stained red. The cells produced in the optimized medium differed from those produced in the basal medium. In the basal medium at 24 h, endospores appeared inside the cells (dark blue arrow, Fig. 2B). Conversely, free

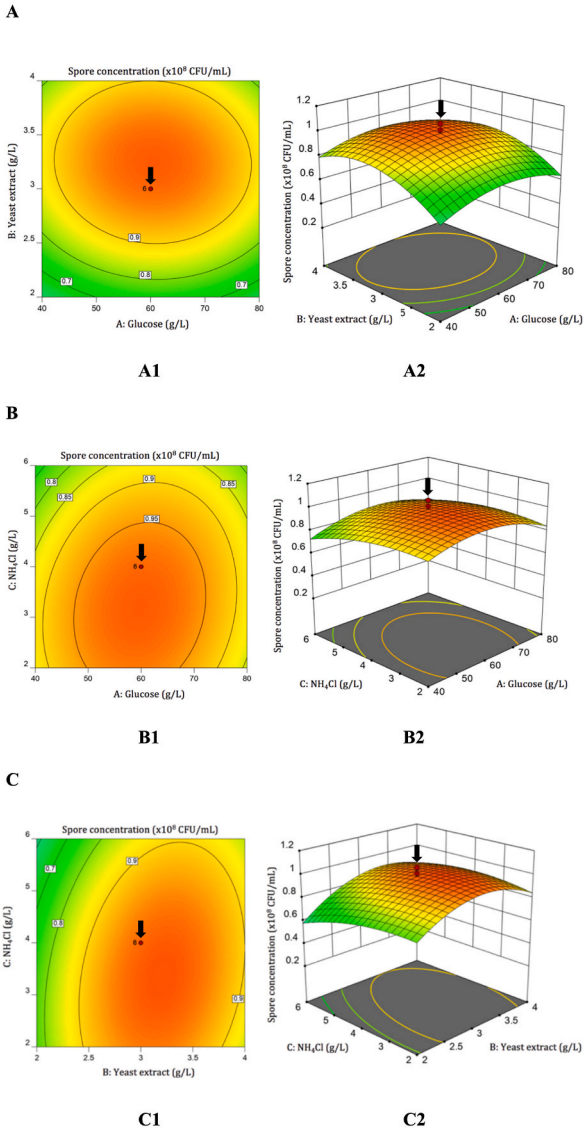

Fig. 1. Concentration effect of glucose, yeast extract, and NH_4Cl during the cultivation of *Bacillus* sp. TL7-3 at 30 °C and 200 rpm represented by using a contour plot and 3-D response surface plot: **A1** (contour plot) and **A2** (response surface plot) display the combined influence of yeast extract and glucose; **B1** (contour plot) and **B2** (response surface plot) indicate the interaction effect of NH_4Cl and glucose; and **C1** (contour plot) and **C2** (response surface plot) show the correlation between NH_4Cl and yeast extract. The red dots (indicated by the black arrows) represent the optimized conditions when cultivating *Bacillus* sp. TL7-3 in the optimized GY medium.

spores were observed within 24 h in the culture grown in the optimized medium (light blue arrow, Fig. 3B). At 3–12 h, the high C:N ratio stimulated vegetative growth. This finding was confirmed by data analysis of vegetative cells using Design Expert software (data not shown). Complete glucose consumption was observed for bacteria grown in basal medium during the first 12 h of culturing (Fig. 2A). The culture grown in the optimized medium exhibited rapid glucose consumption during the initial 12 h compared with the final 12 h (Fig. 3A). After 18 h, glucose was gradually utilized and the corresponding spore numbers approached the overall cell numbers. This suggests that a high C:N ratio promoted vegetative growth at 3–12 h and sporulation at 24 h in *Bacillus* sp. TL7-3. The conventional sporulation medium (DSM) was also used to cultivate *Bacillus* sp. TL7-3 spore production, obtaining only 9.45×10^6 CFU/mL at the end of fermentation (Fig. 4).

2.4. Influence of medium composition on the expression of genes relevant to sporulation

The expression levels of key sporulation genes, including *codY*, *kinA*, *spo0F*, and *spo0A*, were observed during the cultivation of *Bacillus* sp. TL7-3 in the optimized medium compared to that in the basal medium (Fig. 5). Quantitative real-time polymerase chain

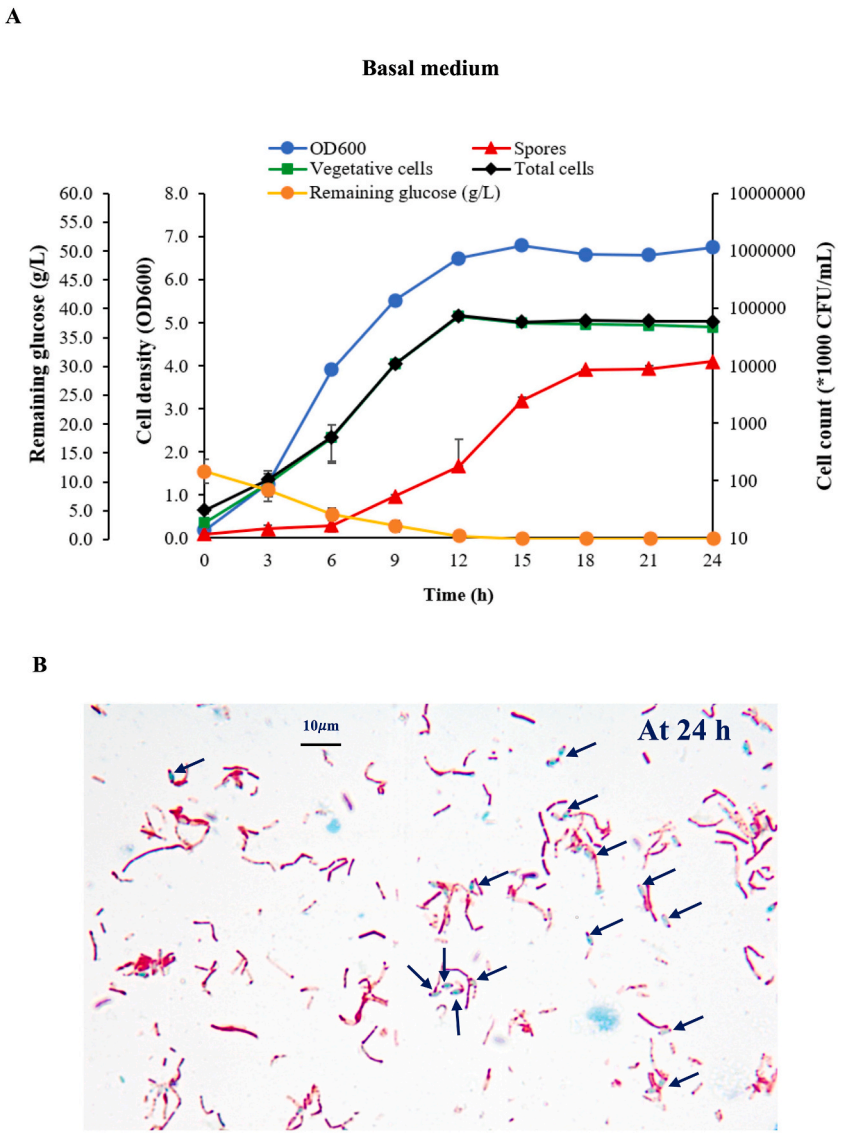

Fig. 2. Growth profile of *Bacillus* sp. TL7-3 cultured in the basal medium at 30 °C and 200 rpm. **(A)** Mean value of three independent biological experiments. The error bars present the standard deviation (±SD). Morphological changes in *Bacillus* sp. TL7-3 grown in the basal medium. **(B)** Cells stained with malachite green and safranin O. The endospores are stained green with malachite and the vegetative cells red with safranin O. The endospores are indicated by the dark blue arrow.

reaction (qRT−PCR) was used to assess differences in relative gene expression levels in cultures grown in the optimized medium compared to the basal medium. Relative expression levels were described using the ΔCt method, employing *hbsU,* the expression level of which remained consistent during cultivation, as a control gene. All the results from the optimized medium were normalized to those obtained from the basal medium. This gene was upregulated when the relative expression level was greater than 1. In contrast, the relative expression level less than 1 suggested that the gene was downregulated. During the early stages of development (1–2 h), the relative expression levels of all genes were similar. At 3 h, the expressions of *spo0A*, *kinA*, and *spo0F* were upregulated, whereas the relative expression of *codY* remained steady. *codY* was strongly downregulated at 6 and 9 h, with the lowest expression observed at 9 h ($p = 0.05$). The relative expression levels of *spo0A*, *kinA*, and *spo0F* peaked at 6 h and then decreased. At 6 and 9 h, the expression of *codY* was considerably different from that of the other three genes at the same time points. The expression of all four genes differed at specific time points. The expression of genes throughout the log phase differed considerably from that during the early growth and stationary phases. After 12 h, as vegetative growth approached the stationary phase, as observed from the trend lines of OD600 (Fig. 2A and 3A), the expression levels of all genes were similar, showing that the expression levels of these genes in the culture grown in the basal medium were identical to those in cells grown in the optimized medium (Fig. 5).

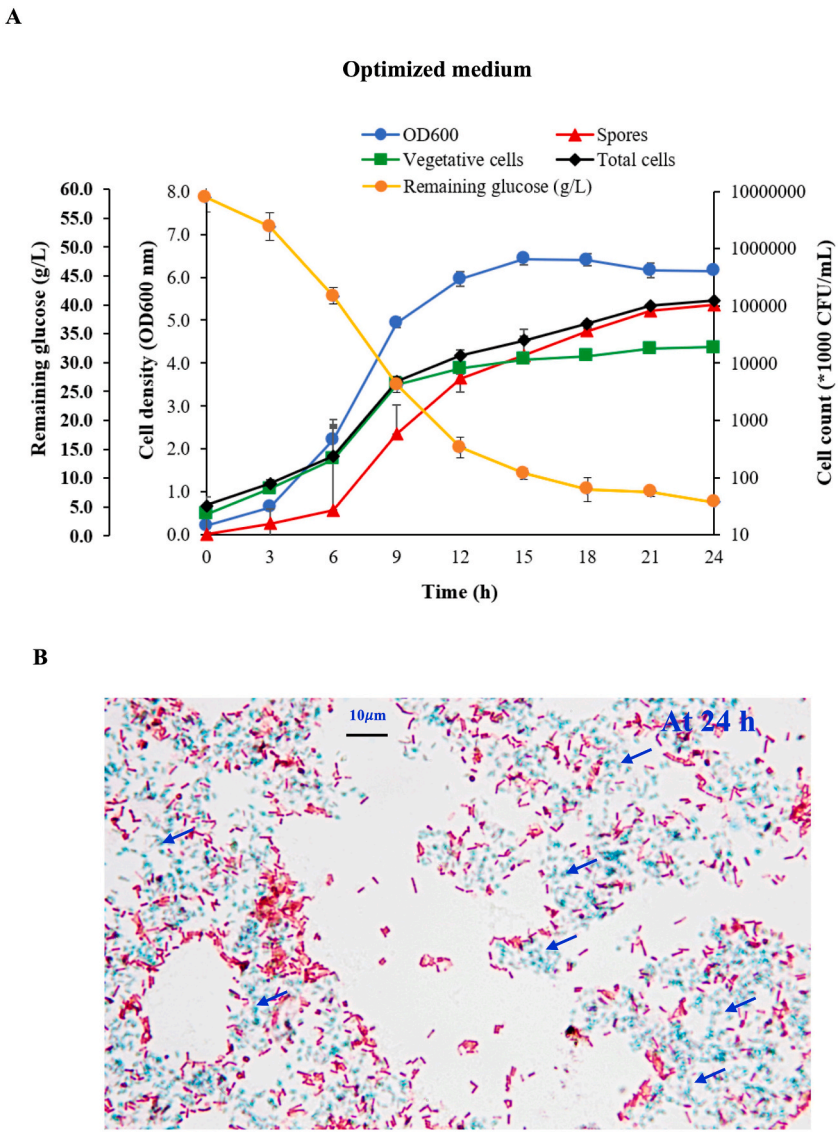

Fig. 3. Growth profile of *Bacillus* sp. TL7-3 cultured in the optimized medium at 30 °C and 200 rpm. **(A)** Mean value of three independent biological experiments. The error bars represent the standard deviation (±SE). Morphological changes in *Bacillus* sp. TL7-3 grown in an optimized medium. **(B)** Cells stained with malachite green and safranin O. The endospores appear green with malachite and the vegetative cells red with safranin O. The free spores are indicated by the light blue arrow.

2.5. Influence of the weight ratio of carbon and nitrogen substrates on GK activity and intracellular GMP, GDP, and GTP level

During culture, the activity of GK was examined together with its enzymatic conversion products (GMP, GDP, and GTP) besides the expression of relevant genes in sporulation pathway (*codY*, *spo0A*, *kinA*, and *spo0F*) (Fig. 6). As the culture progressed to the mid-log phase, the specific activity of GK in both the basal and optimized media increased (referred to as the trend lines of OD600 in Fig. 2A and 3A). Subsequently, GK activity was reduced. When the specific activity of GK was compared during the first hour for the culture grown in the optimized medium, we found that the value was the same as that for the culture grown in basal medium. The specific activity of GK was lower when *Bacillus* sp. TL7-3 cells were grown in the optimized medium with a higher C:N ratio than those grown in the basal medium. This result was more pronounced between 2 h and 6 h ($p < 0.05$).

The amounts of intracellular GMP, GDP, and GTP were further evaluated, as the concentration of these nucleotides is regulated by GK activity (Fig. 6A), which transforms GMP into GDP (Fig. 6B and C). Subsequently, GDP is converted to GTP, which controls the sporulation of *Bacillus* sp. The concentrations of GMP, GDP, and GTP in the culture grown in basal medium were low at 1 and 2 h. At 3 h, the GMP level of the culture in the basal medium was high. GDP and GTP were detected at 3 and 6 h, respectively. GMP, GDP, and GTP concentrations were significantly lower during the cultivation of *Bacillus* sp. TL7-3 cells in the optimized medium. Notably, the

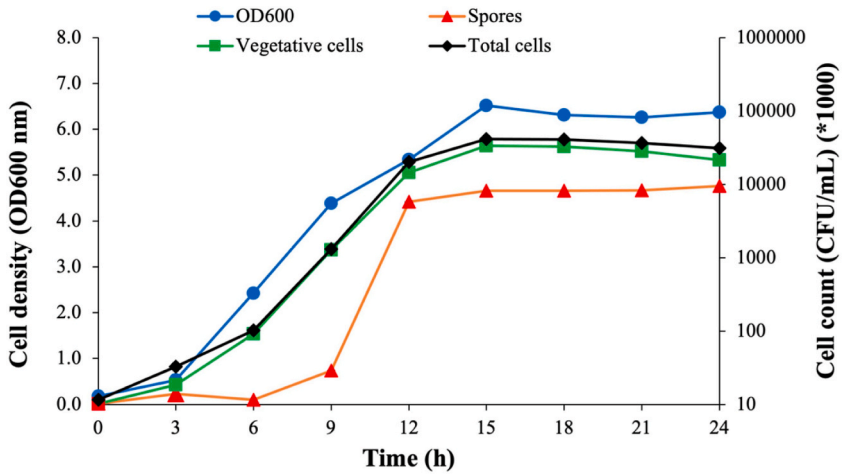

Fig. 4. Growth profile of *Bacillus* sp. TL7-3 cultured in DSM medium at 30 °C and 200 rpm. Mean value of three independent biological experiments. The error bars represent the standard deviation (±SE).

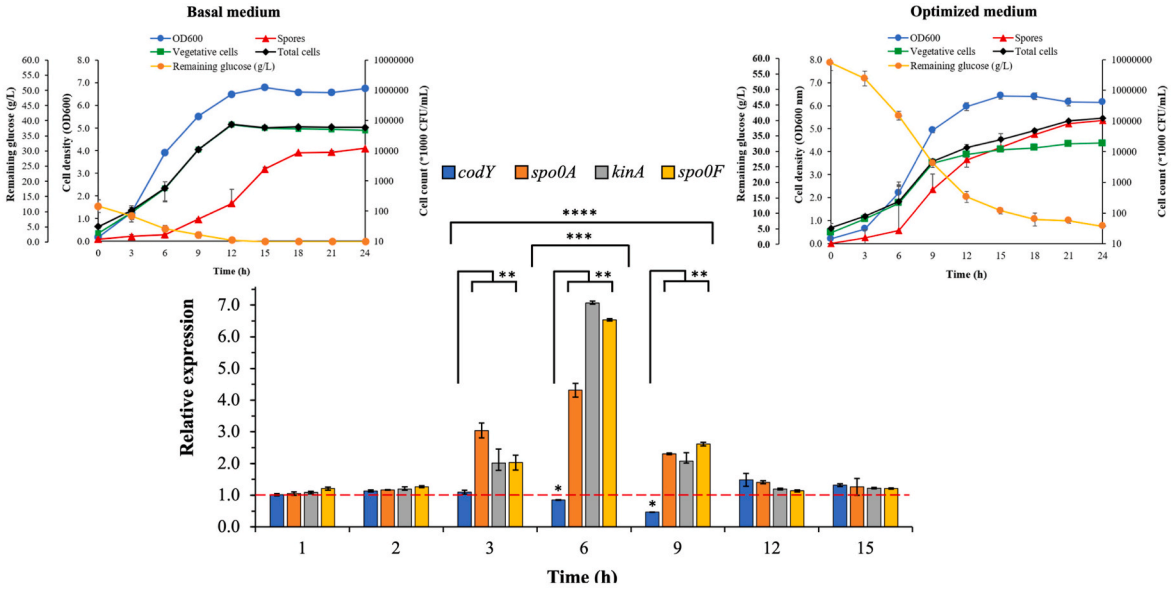

* The expression of *codY* was significantly different from that of *codY* at other time points ($P < 0.05$).

** At the same hour, the expression of *codY* is significantly different from that of other genes ($p < 0.05$)

*** All genes are significantly different from the genes at other time points ($p < 0.05$)

**** The expression levels of *kinA*, *spo0A*, and *spo0F* are significantly different from those of *kinA*, *spo0A*, and *spo0F* at 1, 2, 12, and 15 h ($p < 0.05$)

Fig. 5. Relative expression of *codY* (blue), *spo0A* (orange), *kinA* (gray), and *spo0F* (yellow) during the cultivation of *Bacillus* sp. TL7-3 in an optimized medium compared with cells grown in the basal medium. The relative expression levels were calculated using the ΔCt method and *hbsU* as the housekeeping gene. The ΔCt value of the samples in the optimized medium was normalized to the ΔCt value of those grown in the basal medium. The standard deviations (±SD) were analyzed using three replications of independent biological experiments.

GTP level of the culture in the optimized medium remained low throughout fermentation (Fig. 6D). The low GTP concentration compared to the GMP and GDP concentrations corresponded to the GK activity of *Bacillus* sp. TL7-3 cells were cultivated in the optimized medium. This was evident during the later cultivation periods (12 and 15 h) (Fig. 6).

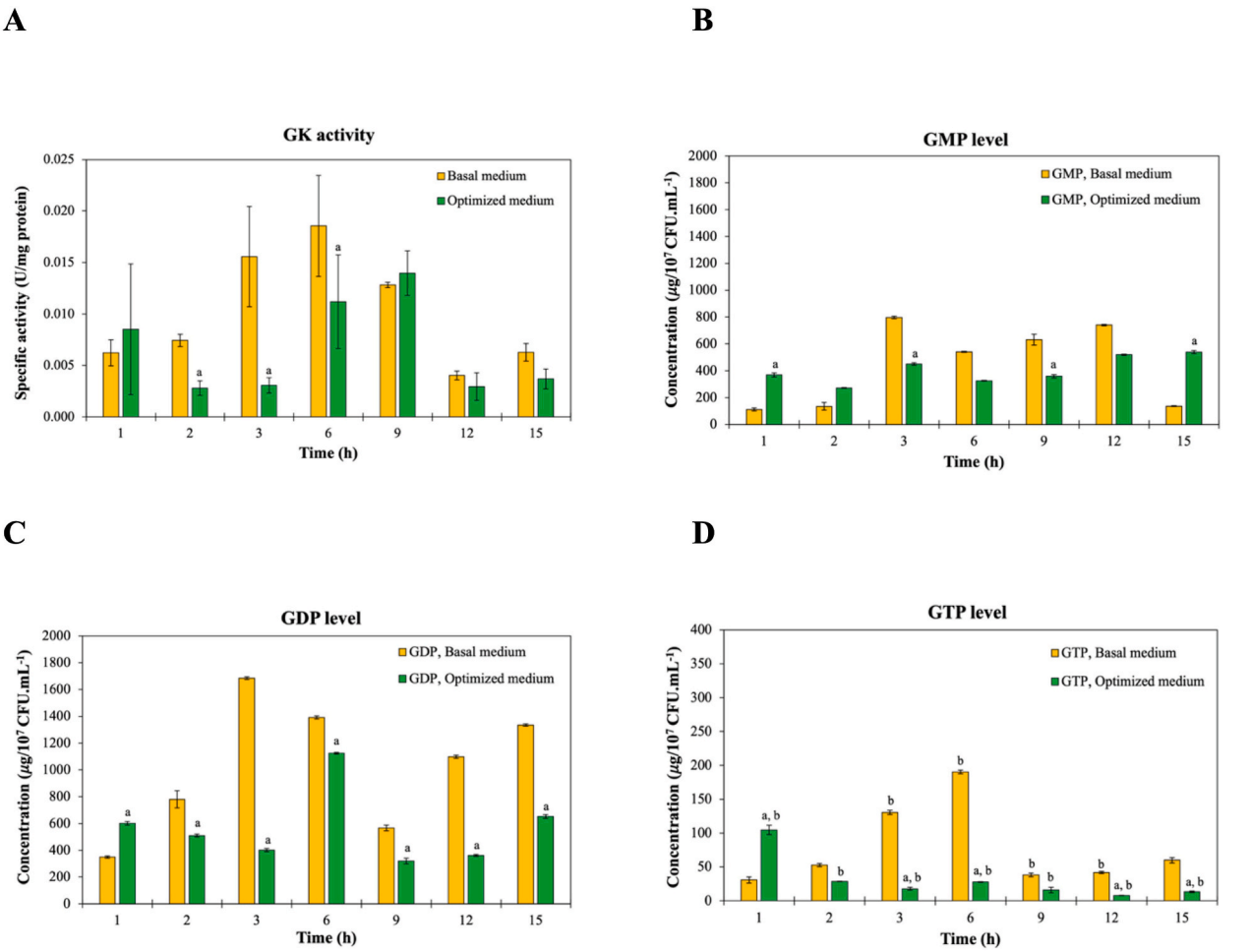

Fig. 6. Enzymatic activity of guanylate kinase (GK) (A) and the level of intracellular GMP (B), GDP (C), and GTP (D) during *Bacillus* sp. TL7-3 cultivation in two different media: basal medium (yellow) and optimized medium (green). The data show the average values of three independent experiments, with the error bars representing ±SD.

3. Discussion

In typical 2-stage fermentation, the preculture seed cultivated in a growth-promoting medium, such as Luria-Bertani broth, is transferred into a spore production medium, such as DSM, at a 10 % inoculum size. Tang et al. (2017) used a 2-stage fermentation process to produce spores. *Bacillus* sp. cells were initially grown in Luria-Bertani broth before being transferred to DSM. The generation time during growth and sporulation was approximately 3 h [3]. The 1-stage fermentation for spore production was attempted in this study. The inoculum size was set to 1 %. The generation time of *Bacillus* sp. TL7-3 was 1.02 h when grown in basal medium and 1.47 h when grown in optimized medium (Fig. S5). Spore formation was also observed during the initial growth stage (first 6 h), although the spore production rate was low (Figs. 2 and 3). The findings of this study and those reported by Tang et al. (2017) implied that the strain, medium composition, and cultivation conditions affected bacterial generation time and spore production. Compared to the typical 2-stage spore production fermentation, the 1-stage fermentation in this study omitted the preculture seed step and required a small inoculum size, thereby lowering the spore production cost. Table 4 compares the cost of the spore production medium used in this study with that of the conventional medium. The cost of the optimized GY medium used in this study was 6.7 times lower than that of the DSM. In terms of the operating procedures, spore production performance, and process cost, the spore production process in this study was cost-effective. In terms of process efficiency, the generation time and spore concentration of *Bacillus* sp. TL7-3 cells grown in DSM medium (1.83 h and 9.45×10^6 CFU/mL) (Fig. 4 and Fig. S5) were lower than those grown in the basal (1.02 h and 1.20×10^7 CFU/mL) (Fig. 2 and Fig. S5) and optimized (1.47 h and 1.05×10^8 CFU/mL) (Fig. 3 and Fig. S5) media. The lowest spore concentration obtained from cultivation in DSM may have been due to glucose deficiency. Glucose serves as the carbon skeleton of cell biomass. High cell concentrations were obtained when sufficient glucose was present. With an appropriate ratio of glucose to nitrogen substrates, vegetative cells transform into spores, resulting in a high spore concentration at the end of cultivation. Therefore, in terms of process efficiency and production cost, the optimized medium obtained in this study provided the best spore production

Table 4
Cost analysis of the spore production medium.

No.	DSM		Chemical price			Price per liter (THB)
	Components	Concentration (g/L)	Price/Unit (THB)	Unit (g)	THB/g	
1	Bacto nutrient broth (Difco)[a]	8	3720	500	7.44	59.520
2	KCl[b]	1	1200	1000	1.20	1.2000
3	$MgSO_4 \cdot 7H_2O$[b]	0.1250	850	500	1.70	0.2125
4	$MnCl_2$[b]	0.0013	700	500	1.40	0.0018
5	$FeSO_4$[b]	0.0002	450	500	0.90	0.0001
6	$Ca(NO_3)_2$[b]	0.1640	600	500	1.20	0.1968
Total price per liter (THB)						61.13
No.	Optimized medium		Chemical price			Price per liter (THB)
	Components	Concentration (g/L)	Price/Unit (THB)	Unit (g)	THB/g	
1	Glucose (950 THB/25 kg)[c]	60	38	1000	0.04	2.28
2	Yeast extract[b]	3	860	1000	0.86	2.58
3	NH_4Cl[b]	4	400	500	0.80	3.20
4	KH_2PO_4[b]	0.25	450	500	0.90	0.23
5	K_2HPO_4[b]	0.25	470	500	0.94	0.24
6	$CaCO_3$[d]	5	48.36	1000	0.05	0.24
7	Salt solution	10 mL/L				0.3176
Total price per liter (THB)						9.08

Notes: Price list available on.
Currency rate on July 15, 2023.
1THB (Thai Baht) = 0.029 USD (United States Dollar).
[a] https://www.mpimpex.co.th (retrieved on July 15, 2023).
[b] https://www.labvalley.com (retrieved on July 15, 2023).
[c] SAC SCI-ENG Ltd., Part. (Retrieved May 23, 2022).
[d] S.M. Chemical Supplies Co., Ltd. (retrieved on May 23, 2022).

performance.

Response surface analysis revealed the interaction effects of carbon (glucose) and nitrogen (yeast extract and NH_4Cl) sources on spore concentrations. The RSM (Eq. (1)) and reliability of the model (Table 3) suggested that yeast extract and NH_4Cl are crucial for spore production. The contour plots revealed that the optimized medium composition that resulted in the highest spore production contained more glucose (60 g/L compared to 10 g/L in the basal medium) but less yeast extract (3 g/L compared to 15 g/L in the basal medium), whereas the concentration of NH_4Cl remained constant. An 8.57-fold increase in the weight ratio of the C:N substrates resulted in an 8.76-fold increase in spore concentration. These data suggest that a higher C:N ratio in the culture medium aided sporulation. In addition, the different C:N ratios of the optimized and basal media influenced not only the spore yield but also the spore-forming characteristics of *Bacillus* sp. strain TL7-3. Microscopic observations confirmed that the optimized medium could stimulate free spores, whereas the cells in the basal medium were still endospores. Based on the investigation of *Clostridium cochlearium* as a potential probiotic, Edirisuriya (2021) determined that free spores could survive in an environment mimicking the pH of the stomach better than endospores [20]. Applying the spore form as a free spore is important for survival under unfavorable digestive conditions. Thus, this study provides knowledge on medium optimization strategies for enhancing the free spores of *Bacillus* sp. strain TL7-3 through the effect of C:N ratios.

Previous research has indicated that glucose concentration significantly impacts spore formation. An appropriate glucose concentration promotes development and increases spore concentration [21]. Liu and Tzeng (2000) investigated the sporulation kinetics of *Bacillus thuringiensis* and the influence of the starting glucose concentration on the initiation of sporulation [22]. In the current study, a high C:N ratio promoted vegetative growth at 3–12 h. Moreover, at 24 h, the glucose content had a weak effect ($p > 0.05$) on the sporulation of *Bacillus* sp. TL7-3; however, the weight ratio of the C:N substrate had a considerable impact on spore formation. These findings are consistent with those published by Gao et al. (2007), who determined that the C:N ratio is more important for sporulation than the carbon content and that the sporulation process is strain dependent [23]. However, as shown in Table 2, an excessive weight ratio of C:N substrates reduced spore formation. Yu et al. (1998) reported results comparable to those of the present study. They found that increasing the C:N ratio to 15:1 enhanced the spore yield but an increase to more than 15:1 resulted in decreased growth and sporulation [24].

Medium with a high concentration of yeast extract promoted growth but not sporulation. A reduction in yeast extract can activate spore formation due to nitrogen starvation during cultivation [22,24]. High salt concentrations inhibit the sporulation of *B. subtilis* at the initial stage of culturing [25]. The steep slopes of the surface plots in Fig. 1 demonstrate that an increase in NH_4Cl concentration lowered the spore concentration. This could be explained by the high salt concentrations, which may have blocked gene activation under the control of *spo0A*, the main gene that regulates sporulation. This hampers the early stages of sporulation [25].

The increasing spore concentration indicated that the optimized medium boosted spore formation compared to the basal medium, which had a lower weight ratio of C:N substrates. This could be further explained by the fact that the expression level of *spo0A* dramatically increased from 3 to 9 h because of *codY* downregulation. During this time, the upregulation of *spo0A* prompted cells in

vegetative growth to enter sporulation, resulting in a higher spore concentration at the end of cultivation. Another study found that boosting *spo0A* expression promoted sporulation [26], supporting the findings of the present study. Spo0A is activated by phosphorylation via a multicomponent phosphorelay that includes a histidine kinase and kinA, which are encoded by the *kinA* gene under positive transcriptional control [6]. KinA activation stimulates the function of Spo0F, which is encoded by *spo0F*. Spo0F further activates Spo0A during phosphorylation [27]. As shown in Fig. 5, the expression levels of *kinA* and *spo0F* were linked to those of *spo0A*. These two genes were significantly expressed from 3 to 9 h, with the maximum relative expression observed at 6 h, similar to that of *spo0A*. Sporulation is also driven by *codY*, which encodes the CodY protein, which functions as a transcriptional regulator of Spo0A. This mechanism is thought to be mediated by intracellular GTP levels. *CodY*-mediated *spo0A* repression is reduced when the GTP pool is lowered [28]. *codY* mutants enhance sporulation in *B. subtilis*, resulting in increased spore counts [29]. The relative expression levels of *codY*, *spo0A*, *kinA*, and *spo0F* in Fig. 5 suggest that the optimized medium composition plays a role in triggering and controlling sporulation in *Bacillus* sp. TL7-3. The results showed that with the correct medium composition, genetic alteration of *codY* did not appear to be essential for increased spore production.

Many studies have shown that a pool of intracellular GTP controls the action of CodY. The binding of intracellular GTP to the metabolic binding domain of CodY results in the correct conformation of this protein, thus activating CodY (Fig. 6). GTP synthesis is controlled by GK, also known as GMP kinase, which is encoded by *gmk*. GK converts GMP to GDP via the GTP biosynthesis pathway. This pathway plays critical roles in the growth, development, and virulence of diverse organisms [21]. In this pathway, phosphoribosyl pyrophosphate (PRPP) is a precursor converted into IMP, GMP, GDP, and GTP [30]. PRPP is initially synthesized from ribose-5-phosphate (R5P) by PRPP synthase, which is encoded by *prs* [31].

The conversion of PRPP to GTP is hampered by nutritional constraints due to the restricted conversion of GMP to GDP as a result of GK inhibition (Fig. 7) [32,33]. Nitrogen limitation increases the production of guanosine 3′,5′-bipyrophosphate (ppGpp) (Fig. 7) [34]. The high ppGpp levels suppressed GK activity; therefore, GMP could not be converted into GDP. Furthermore, a large pool of GMP induces feedback inhibition, resulting in IMP conversion to AMP rather than GMP [35]. This eventually leads to elevated ATP [36]. In addition, high ADP levels regulate *prs* by inhibiting PRPP synthesis [31,35,37]. When PRPP levels decreased, the intracellular levels of histidine, tryptophan, and NAD decreased. This eventually slows growth by inhibiting biosynthesis. When NAD is depleted, KinA is activated, promoting the activation of Spo0A and facilitating sporulation [6,28,38]. Nutritional deprivation during cultivation reduced GK activity and decreased intracellular GTP levels, resulting in the downregulation of *codY*, upregulation of *spo0A*, *kinA*, and *spo0F*, and an increase in the spore count of *Bacillus* sp. TL7-3 cells grown in the optimized medium.

The results indicated that the medium composition, in particular the ratio of carbon and nitrogen sources, played a role in GK inhibition and thus affected GTP regeneration. A low amount of GTP in the optimized medium inactivated CodY, which is a suppressor of *spo0A* transcription, leading to the expression of *spo0A* and subsequent triggering of free spore formation. The promising outcome of using the optimized medium for spore production is a cost-effective process that promotes high free spore generation from low-cost media, thereby serving as an alternative to costly commercial media. The knowledge gained in this study is beneficial for process optimization, especially in large-scale operations.

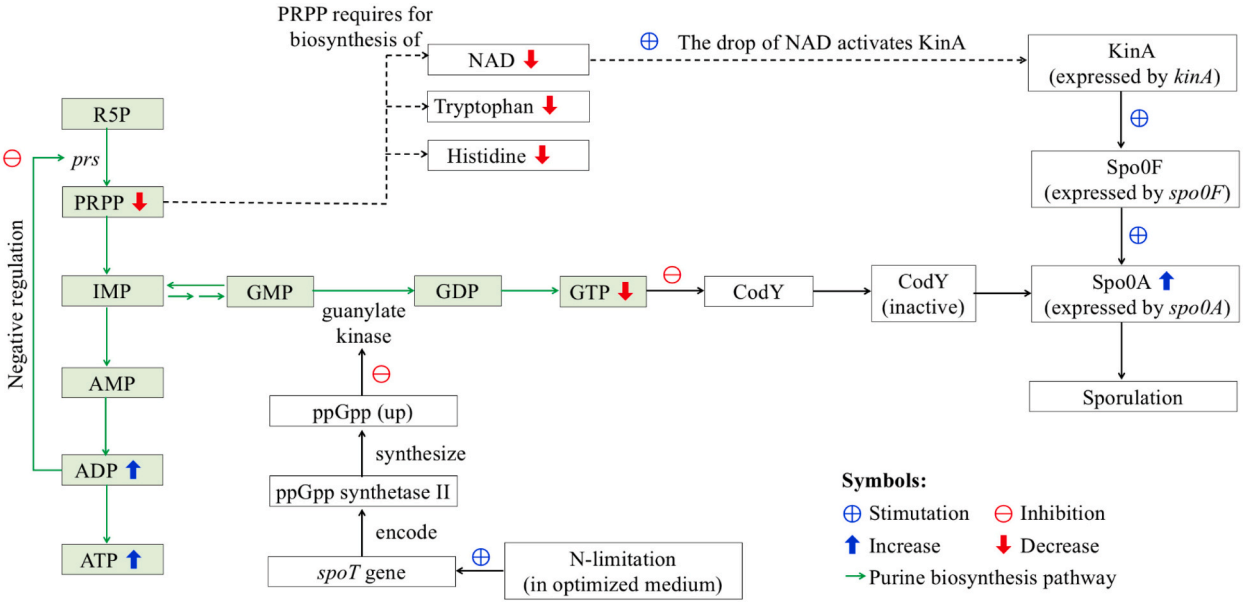

Fig. 7. Purine biosynthesis pathway involving sporulation of *B. subtilis*. *R5P*, ribose-5-phosphate; *PRPP*, 5-phosphoribosyl-1-pyrophosphate; *IMP*, inosine 5′-monophosphate; *ppGpp*, guanosine 3′,5′-bispyrophosphate.

4. Conclusions

Growth patterns, morphological changes, expression levels of relevant genes, and GK activity were investigated in *Bacillus* sp. TL7-3 cultivation in two different media. The findings suggested that the culture medium with the optimized ratio of carbon to nitrogen substrates enhanced vegetative growth at an early stage (log phase) and triggered the onset of sporulation when sufficiently high cell numbers were acquired, which was mandatory for enhancing spore production. Understanding the nutrient consumption rates of carbon and nitrogen sources could reveal further information for improving spore production through medium optimization.

5. Materials and methods

5.1. Bacterial strain, inoculum preparation, media, and culture conditions

The bacterial isolate TL7-3, screened from local Thai fermented soybeans by Professor Somboon Tanasupawat, was used as a model spore-producing bacterium to study key gene expression and GK activity. The bacterium was identified as *Bacillus* sp. TL7-3 via 16 S rRNA gene sequencing. The nucleotide sequence (16 S rRNA gene sequence) was deposited in the NCBI GenBank database under accession number MW820294.

Bacillus sp. TL7-3 was subcultured in a glucose, yeast extract, peptone (GYP) agar slant, and 1 L contained 10 g glucose, 5 g yeast extract, 5 g peptone, 0.25 g KH_2PO_4, 0.25 g K_2HPO_4, 20 g agar, and a salt solution that included 0.4 g $MgSO_4{\cdot}7H_2O$, 0.02 g $MnSO_4{\cdot}5H_2O$, 0.02 g $FeSO_4{\cdot}7H_2O$, and 0.02 g NaCl. One liter of salt solution contained 40 g $MgSO_4{\cdot}7H_2O$, 2 g $MnSO_4{\cdot}5H_2O$, 2 g $FeSO_4{\cdot}7H_2O$, and 2 g NaCl. The pH of the GYP medium was adjusted to 6.8. The cells were harvested after 24 h of incubation and mixed with a sterile 0.85 % NaCl solution. The optical density of the cell suspension was measured at 600 nm and adjusted to 25 nm using 0.85 % sterile NaCl solution. The diluted cell suspension was used as an inoculum. The unoptimized culture medium was used as the basal medium and 1 L contained 10 g glucose, 15 g yeast extract, 4 g NH_4Cl, 0.25 g KH_2PO_4, 0.25 g K_2HPO_4, 5 g $CaCO_3$, and salt solution that included 0.4 g $MgSO_4{\cdot}7H_2O$, 0.02 g $MnSO_4{\cdot}5H_2O$, 0.02 g $FeSO_4{\cdot}7H_2O$, and 0.02 g NaCl. Fermentation was also carried out for conventional spore production using the DSM to compare the growth profile and spore production performance with those of the basal and optimized media developed in this study. The DSM medium (1 L) was composed of 8 g Bacto nutrient broth (Difco), 10 mL of 10 % (w/v) KCl, 10 mL of 1.2 % (w/v) $MgSO_4{\cdot}7H_2O$, 1 mL of 1 M $Ca(NO_3)_2$, 1 mL of 0.01 M $MnCl_2$, and 1 mM $FeSO_4$. NaOH (1 M) was used to adjust the pH of the DSM to 7.6. The culture medium was inoculated with a cell suspension of 1 % inoculum size (0.5 mL) and incubated at 37 °C until the growth reached the stationary phase. Culture broth samples were collected at specific time intervals (every 1–3 h) for further analysis.

5.2. Medium optimization for spore production

RSM was used to optimize the concentrations of glucose, yeast extract, and NH_4Cl in the basal medium for promoting spore production by *Bacillus* sp. TL7-3. A CCD with five coded levels was introduced to determine the optimum levels of three variables: glucose, yeast extract, and NH_4Cl (Table 1). For the three variables, this design was set up as 2^3 factorial designs with eight points augmented with six replications of the center points (all factors at level 0) and six star points (points with an axial distance to the center of one factor, whereas the other two factors were at level 0). The axial distance was set to 1.68 to make this design orthogonal. Twenty experiments were conducted. To develop the regression equation, the test factors were coded according to the following equation (Eq. (2)):

$$x_i = \frac{X_i - X_0}{\Delta X_i} \tag{2}$$

where x_i is the coded value of the independent variable, X_i is the natural value of the (i) independent variable, X_0 is the natural value of the (i) independent variable at the center point, and ΔX_i is the step change value. For the three-factor system, the model equation (Eq. 3) became

$$Y = b_0 + b_1x_1 + b_2x_2 + b_3x_3 + b_{11}x_1^2 + b_{22}x_2^2 + b_{33}x_3^2 + b_{12}x_1x_2 + b_{13}x_1x_3 + b_{23}x_2x_3 \tag{3}$$

where Y is the predicted response; b_0 is the intercept; b_1, b_2, and b_3 are the linear coefficients; b_{11}, b_{22}, and b_{33} are the squared coefficients; and b_{12}, b_{13}, and b_{23} are the interaction coefficients.

Design Expert software (Stat-Ease Inc., version 12, USA) was used to analyze the results. The model permitted evaluation of the effects of the linear, quadratic, and interactive terms of the independent variables on the dependent variable. Three-dimensional surface plots were constructed to illustrate the main and interactive effects of the independent variables on spore yield.

5.3. Determination of glucose and cell biomass

The culture broth sample was mixed with 1 % HCl before centrifugation at 10,000×*g* and 4 °C for 5 min. The supernatant was collected and prepared for glucose analysis by high-performance liquid chromatography. Initially, the supernatant was filtered through a hydrophilic polytetrafluoroethylene membrane and diluted with double-deionized water. Then, 15 μL of diluted particle-free sample was automatically injected (Shimadzu-SIL-20A HT, Japan) into an organic acid analysis column (Bio-Rad, Aminex

HPX-87H ion exclusion organic acid column; 300 × 7.8 mm, Bio-Rad, USA). It was maintained at 45 °C in the column oven (Shimadzu-CTO-20A, Japan) and eluted with 5 mM H_2SO_4 at a flow rate of 0.6 mL/min (Shimadzu-LC-20A, Japan). A refractive index detector (Shimadzu-RID-20A, Japan) was used to detect organic compounds. To determine the sample concentration from the respective peak areas, standards containing 0–2 g/L of glucose were used as references.

The cell pellet was diluted with 1 % HCl before measuring the optical density at 600 nm using a UV–Vis spectrophotometer (Shimadzu-UV-1280, Japan). The total plate count technique was used to determine the total number of cells, vegetative cells, and spores. To determine the total number of cells, the culture broth was serially diluted with sterile 0.85 % NaCl. The diluted sample was plated onto a nutrient agar (NA) plate and incubated at 37 °C for 16–18 h before colony counting. The number of spores in each sample was determined based on the total plate count. The culture broth was subjected to heat shock at 80 °C for 10 min before dilution with sterile 0.85 % NaCl and plating onto an NA plate. The heat-shocked sample was also incubated at 37 °C for 16–18 h before colony counting. The number of vegetative cells present in the culture broth was determined by subtracting the colony-forming units per milliliter (CFU/mL) of the total cell number from the CFU/mL spore number.

5.4. qRT−PCR

The culture broth of basal and optimized medium collected during fermentation at 1, 2, 3, 6, 9, 12, and 15 h was centrifuged at 10,000×*g* and 4 °C for 10 min and the supernatant was discarded. The cell pellet was washed thrice with sterile deionized water before RNA extraction. RNA was extracted from cell samples using an RNeasy Mini Kit (Qiagen, Germany). The extraction protocol has been reported by Jaiaue et al. (2021) [39]. The obtained RNA was subjected to cDNA synthesis using a Precision nanoScriptTM2 Reverse Transcription Kit (Primer Design, UK) according to the manufacturer's protocol. cDNA samples were analyzed using qRT−PCR. The primers used in this study are listed in Table 5.

qRT−PCR was performed in 0.1 mL individual low-profile tubes. Reactions were performed using a 2 × qPCRBIO SyGreen Mix Lo-ROX Kit (PCR Biosystems, USA). Less than 100 ng of cDNA was added to the reaction mixture, which also contained 1 × qPCRBIO SyGreen Mix and 400 nM of forward and reverse primers. The reaction volume was made up to 20 μL using PCR-grade dH_2O. The *hbsU* gene was used as a control to normalize the expression data because its expression level was constant during vegetative growth. The experiment was conducted in triplicates for each sample. Negative (no template) and positive controls were included for each experiment. Dynamic gene expression was quantified using a MyGo Pro Real-time PCR Cycler (IT IS Life Science Ltd., UK) and the results were calculated using the comparative cycle threshold method [40].

5.5. Cell extraction and protein determination

The culture broth was centrifuged at 15,000 rpm and 4 °C for 10 min. The supernatant was discarded and the cell pellets (approximately 10^7 CFU/mL) were washed three times with ice-cold washing buffer containing 0.1 M phosphate buffer (pH 7.0) and 0.1 M potassium phosphate buffer (pH 7.2) at a 1:1 ratio. The cell pellet was washed with a washing buffer to eliminate ions from the culture medium. At the same weight as the cell pellets, glass beads (Sigma, 425–600 mm, 30–40 U S. sieve) were introduced into the reaction mixture containing the cell pellets, followed by adding 0.05 M potassium phosphate buffer (pH 7.2). The mixture was then sonicated using an ultrasonic disruptor UD-201 (TOMY SEIKO) under the following conditions: output level, 6; duty, 60 %; time, 5 min; sonication (turned on) for 45 s, and cooling (turned off) on ice for 30 s. After centrifugation (15,000 rpm, 4 °*C*, 10 min), the supernatant was collected and used as the cell extract. This procedure was performed in an ice bath to prevent protein denaturation. The cell extract was used for the enzyme activity assay and determination of intracellular GMP, GDP, and GTP levels by HPLC. The total protein content was determined using Lowry's method [41].

5.6. GK activity assay

GK activity was assayed according to the protocol developed by Hall and Kuhn (1986) [42]. The reagents were prepared and the procedure was performed accordingly. Briefly, the reaction was performed following the oxidation of NADH to NAD^+ at 340 nm in micromoles per min using lactate dehydrogenase. The assay buffer (2.958 mL) consisted of 64.7 mM Tris (pH 7.5), 47.5 mM KCl, 5.7 mM $MgSO_4{\cdot}7H_2O$, 0.57 mM phosphoenolpyruvate, 0.48 mM EDTA, 0.12 mM NADH, 1.0 mM ATP, 3.4 mM GMP, 35 U pyruvate kinase, and 50 U lactate dehydrogenase. Pure GK enzyme at concentrations between 0.012 and 0.024 U (Sigma) was used as a positive control to verify the activity assay. After the reaction system was tested, GK activity in the cell extract was determined under the reaction conditions previously described using pure GK enzyme. The activity of GK in the cell extract was determined using a calibration plot of absorbance at 340 nm versus the amount of NADH in micromoles. Specific GK activity is expressed in units per milligram of protein. The reactions outlined below illustrate the principles of determining GK activity.

$$GMP + ATP \xrightarrow{GK} GDP + ADP$$

$$ADP + PEP \xrightarrow{PK} ATP + Pyruvate$$

$$GDP + PEP \xrightarrow{PK} GTP + Pyruvate$$

Table 5
Primers used in this study.

No.	Name	Primer sequence (5′-3′)	Target
1	CodY-F	GCA AGA AGC AAA GCT GTC GT	*codY*
2	CodY-R	TCT CCA GCT TTC TGA GTG CG	*codY*
3	Spo0A-F	GAA TCG GTC CTT GCG GAA GA	*spo0A*
4	Spo0A-R	CCG GAA GCT GTT CTT TTG CC	*spo0A*
5	KinA-F	CAA GAG CTG AGC GGA CAG AA	*kinA*
6	KinA-R	GCG GAC TCG GGA GAT TTT CA	*kinA*
7	Spo0F–F	ATT TCA AAA CGC ATG ATA TC	*spo0F*
8	Spo0F–R	GTG AAA ATC ATT TAA CGG TT	*spo0F*
9	HbsU-F	TTC CGG CAA CTG CGT CTT TA	*hbsU*
10	HbsU-R	CGT AAA GGA CGC AAC CCT CA	*hbsU*

$$2\ Pyruvate + 2\ NADH \xrightarrow{LDH} 2\ Lactate + 2\ NAD^{+}$$

GK catalyzes the conversion of GMP and ATP to GDP and ADP, respectively. Both GDP and ADP further react with two molecules of PEP by pyruvate kinase to obtain two molecules of pyruvate. Pyruvate is converted into lactate by lactate dehydrogenase in the presence of NADH. The activity of GK was calculated by monitoring the oxidation of NADH to NAD^+ according to the reaction principle mentioned above.

After cell extraction, the cell extract was separated from the cell debris and used to determine GK activity. Sets of blanks were prepared for individual reaction samples to eliminate reading bias. Blank I was set to eliminate reading errors from other reactions catalyzed by GK. Blank II was set to eliminate background NADH and reading interference of the individual cell extracts. To obtain the reading for Blank I, the cell extract was replaced with deionized water in the reaction mixture, whereas NADH was replaced with deionized water to obtain the reading for Blank II. The oxidation of NADH in blanks and samples was observed by following the absorbance every 1 min for 30 min. The absorbance of Blank I was automatically removed using the programmable software of the spectrophotometer used in this study (Synergy HT, multimode microplate reader, Agilent, USA). The GK activity was determined from the net NADH oxidation.

Net NADH oxidation = Oxidation in sample – Oxidation in Blank I – Oxidation in Blank II

5.7. Analysis of intracellular GMP, GDP, and GTP

The cell extract was initially filtered through a membrane filter (0.22 μm) and diluted with double-deionized water before GMP, GDP, and GTP [43]. Analyses were performed using a Shimadzu HPLC system (Shimadzu, Japan) consisting of a binary solvent delivery system (Shimadzu LC-20AD), temperature-controlled column oven (Shimadzu-CTO-20A), an autosampler injector (Shimadzu-SIL-20A HT), and UV detector (Shimadzu-SPD-20AD). Twenty microliter of crude extract was injected into a Synergi Hydro C_{18} column (250 mm × 4.6 mm, 4.0 μm, Phenomenex, USA) and incubated at 40 °C for chromatographic separation using gradient elution at a flow rate of 0.8 mL/min. The mobile phase consisted of 2 buffers. Buffer A was 25 % methanol containing 50 mM KH_2PO_4 and 5 mM tetrabutylammonium hydroxide adjusted to pH 6.9 with 1 M NaOH and buffer B was deionized water containing 10 mM KH_2PO_4 and 8 mM tetrabutylammonium hydroxide adjusted to pH 6.9 with 1 M HCl. The gradient was set as follows: 0–3 min, 48 % B; 3–15 min, 48–100 % B; 15–20 min, 100 % B; and 20–50 min, 48 % B. The absorption wavelength of the UV detector was 254 nm. GMP, GDP, and GTP concentrations were calculated by comparing the peak areas with standard nucleotides. Sample chromatograms of GMP, GDP, and GTP are presented in Fig. S6 in the Supplementary Material.

5.8. Statistical analysis

Statistical analysis of the triplicate dataset was conducted using SPSS (IBM® SPSS® Statistics version 22, USA). An independent sample *t*-test was used to compare the data. Statistical significance was set at $p < 0.05$.

Data availability

Data are included in the article, supplementary materials, and referenced in article. The nucleotide sequence (16 S rRNA gene sequence) of *Bacillus* sp. TL7-3 was deposited in NCBI GenBank and could be accessed through the accession number MW820294.

CRediT authorship contribution statement

Phetcharat Jaiaue: Writing – review & editing, Writing – original draft, Methodology, Investigation, Formal analysis. **Piroonporn Srimongkol:** Resources, Methodology. **Sitanan Thitiprasert:** Writing – review & editing, Methodology, Funding acquisition, Conceptualization. **Jirabhorn Piluk:** Validation, Methodology, Formal analysis. **Jesnipit Thammaket:** Validation, Methodology,

Formal analysis. **Suttichai Assabumrungrat:** Supervision, Funding acquisition. **Benjamas Cheirsilp:** Supervision, Funding acquisition. **Somboon Tanasupawat:** Resources, Conceptualization. **Nuttha Thongchul:** Writing – original draft, Supervision, Project administration, Methodology, Funding acquisition, Conceptualization.

Declaration of competing interest

The authors declare the following financial interests/personal relationships which may be considered as potential competing interests:Nuttha Thongchul reports financial support was provided by National Research Council of Thailand. Nuttha Thongchul reports financial support was provided by National Science and Technology Development Agency. Suttichai Assabumrungrat reports financial support was provided by Research Chair Professor Grant. Sitanan Thitiprasert reports financial support was provided by Fundamental Research Fund. Benjamas Chiersilp reports financial support was provided by Thailand Research Fund. Phetcharat Jaiaue reports financial support was provided by Development and Promotion of Science and Technology Talents Scholarship Program. If there are other authors, they declare that they have no known competing financial interests or personal relationships that could have appeared to influence the work reported in this paper.

Acknowledgments

This work was partially supported by the National Research Council of Thailand and National Science and Technology Development Agency (NSTDA) [Grant No. P-21-50505], Research Chair Professor Grant provided by the National Science and Technology Development Agency (NSTDA), and Fundamental Research Fund [Grant No. CU_FRB65_BCG(33)_209_61_01], and Thailand Research Fund [Grant No. RTA6280014]. PJ is a recipient of the Development and Promotion of Science and Technology Talents (DPST) Scholarship Program.

Appendix A. Supplementary data

Supplementary data to this article can be found online at https://doi.org/10.1016/j.heliyon.2024.e31956.

References

[1] M.E. Sanders, L. Morelli, T.A. Tompkins, Sporeformers as human probiotics: *Bacillus, sporolactobacillus*, and *brevibacillus*, Compr. Rev. Food Sci. Food Saf. 2 (3) (2003) 101–110, https://doi.org/10.1111/j.1541-4337.2003.tb00017.x.
[2] I. Barák, E. Ricca, S.M. Cutting, From fundamental studies of sporulation to applied spore research, Mol. Microbiol. 55 (2) (2005) 330–338, https://doi.org/10.1111/j.1365-2958.2004.04445.x.
[3] Z. Tang, H. Sun, T. Chen, Z. Lin, H. Jiang, X. Zhou, C. Shi, H. Pan, O. Chang, P. Ren, J. Yu, X. Li, J. Xu, Y. Huang, X. Yu, Oral delivery of *Bacillus subtilis* spores expressing cysteine protease of *Clonorchis sinensis* to grass carp (*Ctenopharyngodon idellus*): induces immune responses and has no damage on liver and intestine function, Fish Shellfish Immunol. 64 (2017) 287–296, https://doi.org/10.1016/j.fsi.2017.03.030.
[4] J. Errington, Regulation of endospore formation in *Bacillus subtilis*, Nat. Rev. Microbiol. 1 (2) (2003) 117–126, https://doi.org/10.1038/nrmicro750.
[5] V. Molle, M. Fujita, S.T. Jensen, P. Eichenberger, J.E. González-Pastor, J.S. Liu, R. Losick, The Spo0A regulon of *Bacillus subtilis*, Mol. Microbiol. 50 (5) (2003) 1683–1701, https://doi.org/10.1046/j.1365-2958.2003.03818.x.
[6] S. Tojo, K. Hirooka, Y. Fujita, Expression of *kinA* and *kinB* of *Bacillus subtilis*, necessary for sporulation initiation, is under positive stringent transcription control, J. Bacteriol. 195 (8) (2013) 1656–1665, https://doi.org/10.1128/JB.02131-12.
[7] P.J. Piggot, D.W. Hilbert, Sporulation of *Bacillus subtilis*, Curr. Opin. Microbiol. 7 (6) (2004) 579–586, https://doi.org/10.1016/j.mib.2004.10.001.
[8] P. Joseph, M. Ratnayake-Lecamwasam, A.L. Sonenshein, A region of *Bacillus subtilis* CodY protein required for interaction with DNA, J. Bacteriol. 187 (12) (2005) 4127–4139, https://doi.org/10.1128/JB.187.12.4127-4139.2005.
[9] M.H. Buckstein, J. He, H. Rubin, Characterization of nucleotide pools as a function of physiological state in *Escherichia coli*, J. Bacteriol. 190 (2) (2008) 718–726, https://doi.org/10.1128/JB.01020-07.
[10] S. Garti-Levi, A. Eswara, Y. Smith, M. Fujita, S. Ben-Yehuda, Novel modulators controlling entry into sporulation in *Bacillus subtilis*, J. Bacteriol. 195 (7) (2013) 1475–1483, https://doi.org/10.1128/JB.02160-12.
[11] T. Inaoka, K. Ochi, RelA protein is involved in induction of genetic competence in certain *Bacillus subtilis* strains by moderating the level of intracellular GTP, J. Bacteriol. 184 (14) (2002) 3923–3930, https://doi.org/10.1128/JB.184.14.3923-3930.2002.
[12] A.R. Han, H.R. Kang, J. Son, D.H. Kwon, S. Kim, W.C. Lee, H.K. Song, M.J. Song, K.Y. Hwang, The structure of the pleiotropic transcription regulator CodY provides insight into its GTP-sensing mechanism, Nucleic Acids Res. 44 (19) (2016) 9483–9493, https://doi.org/10.1093/nar/gkw775.
[13] R. Sen, K.S. Babu, Modeling and optimization of the process conditions for biomass production and sporulation of a probiotic culture, Process Biochem 40 (7) (2005) 2531–2538, https://doi.org/10.1016/j.procbio.2004.11.004.
[14] S. Das, S. Kharkwal, S.K. Pandey, R. Sen, Multi-objective process optimization and integration for the sequential and increased production of biomass, lipase and endospores of a probiotic bacterium, Biochem. Eng. J. 50 (1–2) (2010) 77–81, https://doi.org/10.1016/j.bej.2010.03.006.
[15] E. Chukeatirote, Thua nao: Thai fermented soybean, J Ethn Foods 2 (2015) 115–118, https://doi.org/10.1016/j.jef.2015.08.004.
[16] K. Kulprachakarn, S. Chaipoot, R. Phongphisutthinant, N. Paradee, A. Prommaban, S. Ounjaijean, K. Rerkasem, W. Parklak, K. Prakit, B. Saengsitthisak, N. Chansiw, K. Pangjit, K. Boonyapranai, Antioxidant potential and cytotoxic effect of isoflavones extract from Thai fermented soybean (Thua-Nao), Molecules 26 (24) (2021) 7432, https://doi.org/10.3390/molecules26247432.
[17] T. Wongsurawat, S. Sutheeworapong, P. Jenjaroenpun, S. Charoensiddhi, A.N. Khoiri, S. Topanurak, C. Sutthikornchai, P. Jintaridth, Microbiome analysis of Thai traditional fermented soybeans reveals short-chain fatty acid-associated bacterial taxa, Sci. Rep. 13 (2023) 7573, https://doi.org/10.1038/s41598-023-34818-0.
[18] M. Phinyo, S. Pumma, P. Thinjan, E. Wangkahart, W. Soonthornchai, Effects of dietary fermented soybean meal with Thua nao starter on the growth performance, body composition, and disease resistance against *Aeromonas hydrophila* of Nile tilapia (*Oreochromis niloticus*), Aquac Rep 34 (2024) 101890, https://doi.org/10.1016/j.aqrep.2023.101890.
[19] P. Setlow, A. Kornberg, Biochemical studies of bacterial sporulation and germination. (23) nucleotide metabolism during spore germination, J. Biol. Chem. 245 (14) (1970) 3645–3652. PMID: 4990475.

[20] P. Edirisuriya, Characterization of *Clostridium Cochlearium* as a Potential Probiotic for Obesity Management, vol. 3441, Wayne State University Dissertations, 2021. https://digitalcommons.wayne.edu/oa_dissertations/3441.
[21] Y. Nomura, A. Izumi, Y. Fukunaga, K. Kusumi, K. Iba, S. Watanabe, Y. Nakahira, A.P.M. Weber, A. Nozawa, Y. Tozawa, Diversity in guanosine 3′,5′-bisdiphosphate (ppGpp) sensitivity among guanylate kinases of bacteria and plants, J. Biol. Chem. 289 (22) (2014) 15631–15641, https://doi.org/10.1074/jbc.M113.534768.
[22] B.L. Liu, Y.M. Tzeng, Characterization study of the sporulation kinetics of *Bacillus thuringiensis*, Biotechnol. Bioeng. 68 (1) (2000) 11–17, https://doi.org/10.1002/(sici)1097-0290(20000405)68:1<11::aid-bit2>3.0.co;2-t.
[23] L. Gao, M.H. Sun, X.Z. Liu, Y.S. Che, Effects of carbon concentration and carbon to nitrogen ratio on the growth and sporulation of several biocontrol fungi, Mycol. Res. 111 (1) (2007) 87–92, https://doi.org/10.1016/j.mycres.2006.07.019.
[24] X. Yu, S.G. Hallett, J. Sheppard, A.K. Watson, Effects of carbon concentration and carbon-to-nitrogen ratio on growth, conidiation, spore germination and efficacy of the potential bioherbicide *Colletotrichum coccodes*, J. Ind. Microbiol. Biotechnol. 20 (6) (1998) 333–338, https://doi.org/10.1038/sj.jim.2900534.
[25] C.A. Engelkes, R.L. Nuclo, D.R. Fravel, Effect of carbon, nitrogen, and C:N ratio on growth, sporulation, and biocontrol efficacy of *Talaromyces flavus*, Phytopathology 87 (5) (1997) 500–505, https://doi.org/10.1094/PHYTO.1997.87.5.500.
[26] N. Widderich, C.D.A. Rodrigues, F.M. Commichau, K.E. Fischer, F.H. Ramirez-Guadiana, D.Z. Rudner, E. Bremer, Salt-sensitivity of σH and Spo0A prevents sporulation of *Bacillus subtilis* at high osmolarity avoiding death during cellular differentiation, Mol. Microbiol. 100 (1) (2016) 108–124, https://doi.org/10.1111/mmi.13304.
[27] M. Fujita, J.E. González-Pastor, R. Losick, High- and low-threshold genes in the Spo0A regulon of *Bacillus subtilis*, J. Bacteriol. 187 (4) (2005) 1357–1368, https://doi.org/10.1128/JB.187.4.1357-1368.2005.
[28] P. Eswaramoorthy, D. Duan, J. Dinh, A. Dravis, S.N. Devi, M. Fujita, The threshold level of the sensor histidine kinase KinA governs entry into sporulation in *Bacillus subtilis*, J. Bacteriol. 192 (15) (2010) 3870–3882, https://doi.org/10.1128/JB.00466-10.
[29] N. Mirouze, P. Prepiak, D. Dubnau, Fluctuations in *spo0A* transcription control rare developmental transitions in *Bacillus subtilis*, PLoS Genet. 7 (4) (2011) e1002048, https://doi.org/10.1371/journal.pgen.1002048.
[30] A. Kriel, A.N. Bittner, S.H. Kim, K. Liu, A.K. Tehranchi, W.Y. Zou, S. Rendon, R. Chen, B.P. Tu, J.D. Wang, Direct regulation of GTP homeostasis by (p)ppGpp: a critical component of viability and stress resistance, Mol Cell 48 (2) (2012) 231–241, https://doi.org/10.1016/j.molcel.2012.08.009.
[31] B. Wang, R.A. Grant, M.T. Laub, ppGpp coordinates nucleotide and amino-acid synthesis in *E. coli* during starvation, Mol Cell 80 (1) (2020) 29–42.e10, https://doi.org/10.1016/j.molcel.2020.08.005.
[32] M. Ratnayake-Lecamwasam, P. Serror, K.W. Wong, A.L. Sonenshein, *Bacillus subtilis* CodY represses early-stationary-phase genes by sensing GTP levels, Genes Dev. 15 (9) (2001) 1093–1103, https://doi.org/10.1101/gad.874201.
[33] K. Liu, A.R. Myers, T. Pisithkul, K.R. Claas, K.A. Satyshur, D. Amador-Noguez, J.L. Keck, J.D. Wang, Molecular mechanism and evolution of guanylate kinase regulation by (p)ppGpp, Mol Cell 57 (4) (2015) 735–749, https://doi.org/10.1016/j.molcel.2014.12.037.
[34] K.L. Nawrocki, A.N. Edwards, N. Daou, L. Bouillaut, S.M. McBride, CodY-dependent regulation of sporulation in *Clostridium difficile*, J. Bacteriol. 198 (15) (2016) 2113–2130, https://doi.org/10.1128/JB.00220-16.
[35] L.M. Wick, T. Egli, Molecular components of physiological stress responses in *Escherichia coli*, Adv. Biochem. Eng. Biotechnol. 89 (2004) 1–45, https://doi.org/10.1007/b93957.
[36] T. Shi, Y. Wang, Z. Wang, G. Wang, D. Liu, J. Fu, T. Chen, X. Zhao, Deregulation of purine pathway in *Bacillus subtilis* and its use in riboflavin biosynthesis, Microb. Cell Factories 13 (1) (2014) 101, https://doi.org/10.1186/s12934-014-0101-8.
[37] K.F. Jensen, G. Dandanell, B. Hove-Jensen, M. WillemoËs, V. Stewart, Nucleotides, nucleosides, and nucleobases, EcoSal Plus 3 (1) (2008), https://doi.org/10.1128/ecosalplus.3.6.2.
[38] S. Tojo, K. Kumamoto, K. Hirooka, Y. Fujita, Heavy involvement of stringent transcription control depending on the adenine or guanine species of the transcription initiation site in glucose and pyruvate metabolism in *Bacillus subtilis*, J. Bacteriol. 192 (6) (2010) 1573–1585, https://doi.org/10.1128/JB.01394-09.
[39] P. Jaiaue, P. Srimongkol, S. Thitiprasert, S. Tanasupawat, B. Cheirsilp, S. Assabumrungrat, N. Thongchul, A modified approach for high-quality RNA extraction of spore-forming *Bacillus subtilis* at varied physiological stages, Mol. Biol. Rep. 48 (10) (2021) 6757–6768, https://doi.org/10.1007/s11033-021-06673-7.
[40] K.J. Livak, T.D. Schmittgen, Analysis of relative gene expression data using real-time quantitative PCR and the 2ˆ(-delta delta CT) method, Methods 25 (4) (2001) 402–408, https://doi.org/10.1006/meth.2001.1262.
[41] O.H. Lowry, N.J. Rosebrough, A.L. Farr, R.J. Randall, Protein measurement with the folin phenol reagent, J. Biol. Chem. 193 (1) (1951) 265–275, https://doi.org/10.1016/s0021-9258(19)52451-6.
[42] S.W. Hall, H. Kühn, Purification and properties of guanylate kinase from bovine retinas and rod outer segments, Eur. J. Biochem. 161 (3) (1986) 551–556, https://doi.org/10.1111/j.1432-1033.1986.tb10477.x.
[43] C. Zhang, Z. Liu, X. Liu, L. Wei, Y. Liu, J. Yu, L. Sun, Targeted metabolic analysis of nucleotides and identification of biomarkers associated with cancer in cultured cell models, Acta Pharm. Sin. B 3 (4) (2013) 254–262, https://doi.org/10.1016/j.apsb.2013.06.002.